The Space Congress® Proceedings

1968 (5th) The Challenge of the 1970's

Apr 1st, 8:00 AM

A Second Generation (High-Speed) Maximum Power Tracker for Space Applications

Clement A. Berard

Radio Corporation of America, Astro-Electronics Division, Prince ton, New Jersey

Follow this and additional works at: https://commons.erau.edu/space-congress-proceedings

Scholarly Commons Citation

Berard, Clement A., "A Second Generation (High-Speed) Maximum Power Tracker for Space Applications" (1968). *The Space Congress® Proceedings*. 1.
https://commons.erau.edu/space-congress-proceedings/proceedings-1968-5th/session-15/1

EMBRY-RIDDLE
Aeronautical University™
SCHOLARLY COMMONS

A SECOND-GENERATION (HIGH-SPEED) MAXIMUM POWER TRACKER
FOR SPACE APPLICATIONS

Clement A. Berard, Jr.
Radio Corporation of America
Astro-Electronics Division
Princeton, New Jersey

Abstract

During the past few years, considerable effort has been exerted by both industry and government to improve the performance of space power systems. One of the significant advances has been the development of practical Maximum Power-Point Tracking (MPPT) systems. This paper presents the background and evolution of a second-generation (high-speed) MPPT system capable of operation with solar arrays with rapidly fluctuating parameters due to mission operation (e.g., spin-stabilized spacecraft).

An experimental model of the high-speed MPPT system has been constructed and tested. Results from these tests are presented herein.

The second-generation MPPT system provides a means of efficient power conditioning that can result in significant increases over conventional systems in space-power system capability. Of additional importance is the applicability of the basic technology to all types of spacecraft, and the wide variety of power-system configurations with which the high-speed MPPT system concept may be employed.

Introduction

The need for Maximum Power-Point Tracking power systems arises as a result of the disadvantages of the conventional systems. Figure 1 shows a typical space power system for an earth-orbiting satellite, which can normally have orbit periods of 90 to 120 minutes; sun-time/occultation ratios of 2-to-1 are common for systems of this type.

Ideally, during the sunlit portion of an orbit, all available energy from the array would be delivered, either to spacecraft loads through an efficient non-dissipative load bus regulator, or to charge the battery through appropriate battery charge-control and protection circuits. During the dark portion of the orbit, energy stored in the battery during the charge cycle is delivered to the load. Proper design ensures energy balance during the lifetime of the spacecraft.

Consider the limitations associated with the commonly used power system configuration. As the array emerges from the Earth's shadow, the low solar-array temperature drives the maximum-power point to a voltage far in excess of the operating voltage range (determined by the battery charge voltage limits) for which the conventional system is customarily designed. The quiescent operating point is at a level far below the potential power capability of a cold-cell array. The advantage of operating the array in the constant-current region and having nearly the same current flow at the array output, but at a much higher voltage level is not realized. Figure 2, based on actual data for an earth-orbiting spacecraft, typifies the situation. The upper line on the graph indicates maximum available power during the satellite day. The dotted line indicates (optimistically) the maximum power extracted from the array by the conventional system. The shaded area represents wasted energy that could be used to supply additional loads, or that could be stored in the battery. Normally, the array generates more power than can be absorbed by the loads and battery and the excess is absorbed either in the charge controller or in a specially designed excess-power dissipator. The resulting spacecraft thermal balance problem, caused by the large amounts of power that may have to be dissipated, becomes particularly severe where there is a large difference between the beginning-of-life and end-of-life array output.

The application of recent advances in power-conditioning technology will substantially increase spacecraft life, or load capability, and decrease the thermal balance problem, by ensuring an optimum source-to-load energy transfer. The concept of Maximum Power Point Tracking involves the delivery of maximum available source power to the spacecraft, regardless of source variations caused by environment or time. Optimum energy transfer results from the adaptive control of pulse-width-modulation (PWM) power-conditioning circuits to effectively match the input impedance of the spacecraft to the output impedance of the solar array at its maximum power point. The spacecraft storage system plays an important role in that any instantaneously available array energy not immediately required for spacecraft loads is delivered to storage. Storage overcharge control, which is fully automatic, is achieved by overriding the maximum power-point tracking control and intentionally mismatching the system and array impedances to produce a less-than-optimum transfer of power. Load demand is always accomplished on a preferential basis. Use of this mismatching technique completely obviates the need for an excess-power

dissipator, such as a shunt regulator, and eliminates the severe thermal-balance problem.

Maximum Power Point Tracking Technique

The operation of MPPT systems is based on the use of pulse-width-modulation techniques to attain source-to-load impedance matching and, therefore, maximum power transfer. The solar-array operating point can be varied by changing the load impedance as illustrated by Figure 3. Implementation of an MPPT system utilizes a PWM device which is, in effect, a d-c impedance

transformer capable of making a single load resistance appear as an infinitely variable load to the source.

The impedance transformation properties of the PWM device can be derived with the aid of Figure 4. Here, the switch opens and closes at a repetition rate of frequency, f. The ratio of closure time, t_{ON}, to the period, T, is the duty-cycle, α, which is controllable.

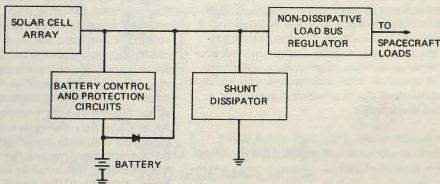If the average power delivered to R_L is the d-c power P_O, then

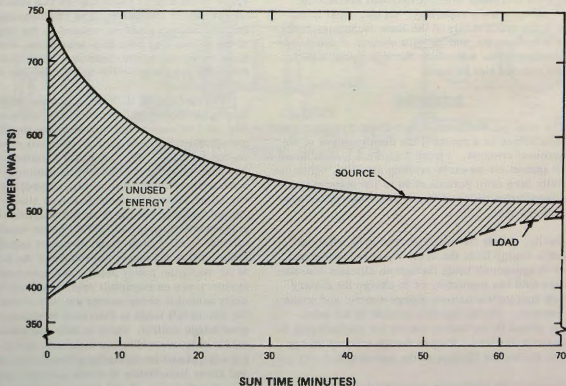Figure 1. A Typical, State-of-the-Art, Solar Power System

Figure 2. Maximum Available Array Power and Power Utilized by a Conventional Power System vs Sun Time

$$R_m = \frac{(V_S)^2}{P_S} \qquad (1)$$

where:

P_S is the power delivered by the source, and
R_m is the effective input resistance;

but if the switching network is essentially non-dissipative, then

$$P_S = P_O = \frac{(V_O)^2}{R_L} \qquad (2)$$

and

$$R_m = \frac{(V_S)^2}{(V_O)^2} R_L \qquad (3)$$

However, if the filter, $L_1 C_1 CR_1$, is an averaging filter, then

$$V_O = \alpha V_S \qquad (4)$$
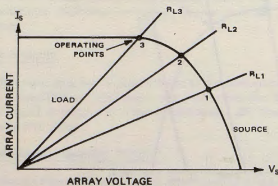
or

$$V_S = \frac{V_O}{\alpha}$$

Therefore,

$$R_m = \frac{V_O^2 R_L}{V_O^2 \alpha^2} = \frac{R_L}{\alpha^2} \qquad (5)$$

Thus, controlling the duty-cycle of a PWM device will control its input impedance as shown graphically in Figure 5 and will provide operating-point control as a function of α.

Assuming the PWM to be essentially non-dissipative as before,

$$P_O \approx P_S \qquad (6)$$

and the array power is then delivered to the load resistor.

By selecting R_L to intersect the $I_S - V_S$ characteristic at a voltage lower than the maximum power voltage (V_p max), an α can be found that will result in maximum array power being delivered to R_L (this condition is $\alpha = \alpha_1$, in Figure 5).

Substitution of a low-impedance load, such as a battery, does not change the control capability. In this case, the output voltage is equal to the battery terminal voltage. The voltage presented to the source side of the switch becomes

$$V_S = \frac{V_B}{\alpha} \qquad (7)$$

The battery voltage, when reflected to the PWM input terminals as modified by the duty-cycle, α, is shown in Figure 6 for values of α less than 1.0.

By selecting V_B to be lower than the maximum-power voltage of the array, an α can be found such that maximum source power will be delivered to the battery (this condition is $\alpha = \alpha_1$, in Figure 6).

Therefore, a sensing and control system that controls α so that load (or source) power is maximized acts as a Maximum Power Point Tracker.

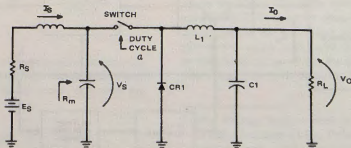Figure 3. Variation of Operating Point with Load

Figure 4. Simplified Schematic of the Basic PWM Circuit

System Background

The first-generation (low-speed) MPPT system operated on the principle of slowly varying the operating point of the source to locate the maximum-power point. The sensing mechanism measures MPPT output current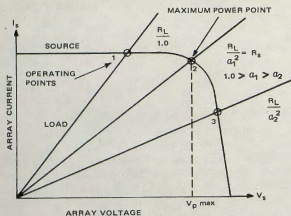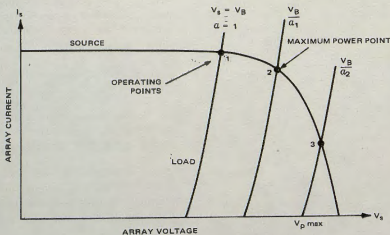 and utilizes the current multiplication properties of the constant-frequency, pulse-width-modulated transistor switch to locate and track the maximum-power point.

A simplified block diagram is shown in Figure 7. Since the output power is proportional to the output current, it is sufficient to maximize the output current to attain maximum power transfer. There are several limitations inherent in this system that restrict its usefulness. Among these are susceptibility to load transients and inability to detect the maximum-power point under certain load conditions. The application of the system is also limited by its slow speed of response to spacecraft having slow array variations (e.g., oriented solar arrays). The laboratory model is capable, however, of operating at source powers up to 1000 watts, source voltages up to 100 volts, with eight independently controlled, parallel, output channels, and with a power-transfer-efficiency exceeding 90 percent.

The low-speed MPPT system is fully capable of affording all the advantages associated with maximum-power-point-tracking space-power systems when applied within its limitations.
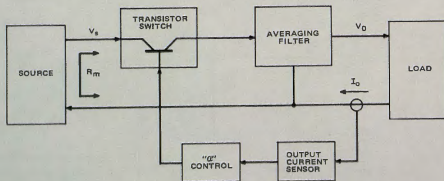
Figure 5. PWM Control of Effective Load Line

Figure 6. PWM Control of Battery Type Load Line

Figure 7. System Diagram — Basic Low-Speed MPPT

Second-Generation-System Concept

Derivation of a high-speed maximum-power tracking system concept must, as a result of the problems and limitations previously described, represent a departure from the slow-scanning and constant-frequency, variable-duty-cycle, pulse-width-modulation methods heretofore employed. The second generation MPPT system is based on an extension of the concepts and techniques developed for ripple-controlled PWM voltage regulators.

The basic system as shown in Figure 8 includes only the functional elements required for the power-tracking mode of operation. The characteristics of some of the functional elements are as follows:

Source

The source power-voltage characteristic obtained at the highest switching frequency of the system must be essentially the same as that at d-c.

Multiplier

The inputs are instantaneous source-voltage and current. The output signal is proportional to the instantaneous source power being delivered. The response time of this element must be compatible with the maximum operating (switching) frequency of the system.

Peak Detector

The input is a signla proportional to the instantaneous source power. The output is a pulse whenever the input signal decreases by a small increment, ΔP, from the previous value.

Pulse Absence Detector (PAD)

The PAD generates an output pulse similar to the peak-detector output whenever the period between peak-detector output pulses exceeds some predetermined time (2 milliseconds). The purpose of this function is to avoid a situation whereby the system might "hang up" in an undesirable state with the power switch either full on or full off.

Toggle

This is a bistable device that changes states with each input pulse. In one state, the toggle drives and holds the power switch on; in the other, it drives and holds the switch off.

Load

The only restriction placed upon the load is that it must be capable of absorbing maximum source power

at some voltage, V_L, which is lower than that at which the source deliveres its maximum power, $V_{P\ max}$.*

Operation of the basic system in the power tracking mode is as described in the following:

Assume that the system is at rest with the source at open-circuit voltage ($V_S = V_{C1} = V_{SOC}$, the source open-circuit voltage) and the power switch open. The opposite assumption (i.e., that the switch is closed and $V_S = V_{C1} = V_L$) can also be made, with the result that the system will start and continue to operate properly. This assumption then, in no way limits the generality of the following description. The PAD will generate a pulse, since the peak detector cannot detect with the system at rest because the source power cannot change. This will then cause the switch to turn on and the switch current, I_{SW}, will begin to flow, increasing at a rate dependent upon V_S and V_L (for a given inductance value of L1). The source voltage will begin to decrease and the source current to increase. In effect, the source operating point will move over the $P_S - V_S$ characteristic toward the maximum power, P_{max}, point. Note that during this time, I_{SW} is composed of I_S and I_{C1} and is greater than either. Note also, that the period of time during which this entire action occurs is consistent with and dependent upon the circuit constants of L1 and C1 and the existing voltage levels. This indicates that the scanning action can be designed to take place in tens or hundreds of microseconds, providing the source can accommodate such high operating rates.

As the source operating point traverses the maximum power point ($V_S = V_{Pmax}$) the source power peaks and then falls off. When P_S decreases from P_{max} by an increment, ΔP, the peak detector generates an output pulse that causes reversal of the state of the power switch and thereby changes the state of the power switch (i.e., turns it off).

At this point in the cycle, two things occur: (1) the current flowing in L1 tends to continue flowing due to its inductance and, as a result, a flyback action occurs causing CR1 to conduct. (2) Source current will be diverted from the power switch and will flow into the capacitor, C1. This will charge the capacitor and cause its voltage (and the source operating point) to rise towards the source open-circuit voltage, V_{soc}. As V_S traverses the maximum power point, V_{Pmax}, source power will again peak (note that P_S is being delivered to the capacitor). When the power decrease (ΔP) is traversed, the peak detector again generates an output

* This voltage requirement is a function of the power switch, inductor (L1), flyback-diode (CR1) configuration, only. Other voltage relationships could be incorporated by utilizing the same basic concept and other voltage-conversion circuitry.
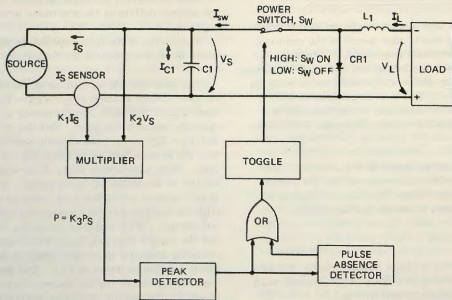
Figure 8. System Diagram — Basic High-Speed MPPT

pulse. This pulse causes reversal of the toggle, causing the power switch to again turn on and the hunting oscillation continues as before. Note that if L1 has a sufficiently large inductance, it will maintain conduction of CR1 through the entire off period of the power switch, although this is not a necessary condition for operation of the system. The system operating frequency will vary from 1 KHz to 8 KHz depending upon the source power.

This MPPT concept will allow maximum power to be drawn from the source, regardless of variations in source characteristics, over a wide range of source variation rates. For example, the high-speed MPPT system is applicable to a solar array having a rapidly fluctuating output. This is the case for a spin-stabilized spacecraft with a body-mounted solar array, which might exhibit ripple in the array power-time characteristic due to the spacecraft rotation. Similarly, source fluctuations due to loading at the source terminals (other than the MPPT loading) will also be followed in a stable manner if the MPPT system operating frequency is sufficiently in excess of the transient rates.

Load Protection Functions

In order to apply the basic MPPT concept to an operating power system, the inclusion of load protective functions is required. The application for which the MPPT system was originally developed is the Nimbus Meteorological Satellite, which included eight nickel-cadmium batteries for energy storage. Thus, the MPPT protection functions are oriented towards battery loads; however, resistive loads do not change the system operation. These functions (including

battery voltage and current limiting, battery high-temperature cut-off, and battery charge current-sharing) are performed by logic and sensing circuitry which is interposed between the toggle and the power switch (Figure 8). System corrections are effected by duty-cycle modification.

Tailoring the MPPT system towards a modular concept (i.e., Nimbus) has led to the designations "Control Unit" and "Battery Module". The Control Unit contains the power sensor, peak detector, PAD, and toggle controls. Each Battery Module consists of a power switch, averaging filters, and load protection controls. An "n" channel system would be composed of one Control Unit and "n" parallel Battery Modules.

If the system is operating in the power-tracking mode, the output current-sharing controls are functioning; the power switches in all the Battery Modules are turned on by the toggle signal from the Control Unit. When the toggle reverses its state, the power switches turn off sequentially; i.e., the switch in the module passing the highest current turns off first, with the others following in the order of decreasing output current. This action modifies (increases) the duty cycle of the individual modules to provide a dynamic control, which tends to equalize the parallel output currents. Current sharing is maintained within a reasonable tolerance, regardless of the variations in load (battery) characteristics.

Battery-protection controls for each module function independently. An error signal is generated within a module if (1) the battery current exceeds a

predetermined maximum value (current limiting), (2) the battery temperature increases above a predetermined maximum limit (high-temperature cutoff), or (3) the battery voltage and temperature increase beyond a predetermined characteristic. The resulting action reduces the duty cycle of the particular module until the battery-protection error signal(s) is reduced to an acceptable level.

Note that the transition from the normal (or tracking) mode to a protected mode, and between various protected modes, is automatic and can be performed continuously.

High-Speed MPPT Circuits

The implementation of the high-speed MPPT concept required the development of many control circuits. It should be noted that the system implementation, as described herein, was intended to demonstrate concept feasibility and that the results may not reflect the optimum circuit configuration. Three of the more unique circuits will be described.

Power Switch Drive Circuitry

A power-switch-drive circuit capable of operation with MPPT input voltages as high as 100 volts d-c was developed for this application. As shown in Figure 9, transistors Q1 and Q2 and associated components comprise the power handling circuits.

Q1 switches load power and Q2 serves to alternately inhibit and enable Q1, as dictated by the output of the pulse-width-modulator. Base drive for Q1 and Q2 is provided by the square-wave inverter through transformers T1A and T1B. Inductor L1 is used to remove inverter switching transients from the base drive of Q1.

The primary windings of transformers T1A and T1B are connected in series. The voltage impressed across terminals A-B will be shared between T1A and T1B in proportion to the effective (reflected load) impedance at the respective primaries. Switching of base drive to Q1 is achieved through control of this voltage-sharing property.

Transistors Q3 and Q4 serve to short circuit windings 5-6 of T1A and T1B respectively, depending upon the state of the pulse-width-modulator output. When Q3 is saturated (Q4 Off), winding 5-6 of T1A is effectively short-circuited, thereby presenting a low impedance at the primary of T1A. Since Q4 is off, a higher impedance is presented at the primary of T1B which is equal to the reflected load of its secondary circuits, causing the major portion of the primary voltage (V_{A-B}) to be impressed upon T1B and its secondary load. This, then, applies base current to Q1 from the inverter, causing it to turn on. Since T1A is essentially short-circuited, there is no drive applied to the base of Q2. Therefore, Q2 is off and its collector

circuit will not divert base drive from Q1. When the pulse-width modulator changes its output state, Q3 turns off and Q4 turns on. This action diverts V_{A-B} from T1B to T1A with the net effect that Q2 is turned on and Q1 is turned off.

Application of this circuit configuration, in place of a d-c coupled circuit, does not degrade the power transfer efficiency. However, no power is dissipated in supplying drive current at the power-switch high-voltage level, due to the magnetic coupling provided by transformer T1. This tends to increase the over-all system efficiency, especially at high-input-voltage conditions.

Power Sensor

One of the more significant requirements imposed on the MPPT circuits is that of sensing and producing a signal proportional to instantaneous array power, with a response time compatible with system speed. While there is no severe accuracy requirement, the power sensor output must be monotonically related to its input and must operate efficiently in that insertion and operating losses must be small relative to the measured power.

The simplified diagram of such a sensor is shown in Figure 10. An array voltage-to-current converter is used to drive the Hall element input to reduce the power required to sense voltage. Array current is applied directly to its load input. The Hall output is then amplified to provide adequate signal level to the peak detector. The existing parameters for the power sensor are:

Source Voltage 0 to 100 volts d-c
Source Current 0 to 20 amperes d-c;

or a maximum source power of 2000 watts. Thus, this sensor would be usable for solar array power sources up to about 1800 watts and at frequencies up to 50 Khz.

Peak Detector

Control of the source (solar array) operating point is accomplished by detecting the maximum source power. The peak detector shown in Figure 11 provides this capability.

Assume the initial conditions are that Ps = 0 and the memory capacitor, C, is discharged. As the operation begins, the source power must be increasing as previously described. V_{in} is also increasing so that the voltage polarities are as shown. Thus, CR1 is forward biased and difference amplifier No. 2 is on, causing C to be charged to V_{in} volts. This continues so long as V_{in} increases. If the instantaneous source power decreases by an increment ΔP, then the voltage polarities reverse, forward-biasing CR2 and triggering the Schmitt
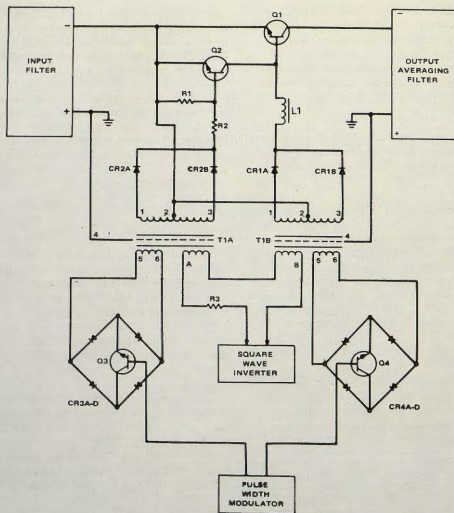
Figure 9. Power-Switch Drive, Schematic Diagram

trigger. This provides a peak detector output pulse and causes the reset switch to close, discharging the memory capacitor.

Operation of this detector with the above power sensor results in a sensitivity (ΔP) which is less than one percent of the maximum source power.

Experimental Model

To demonstrate the validity of the high-speed MPPT concept and the feasibility of the proposed control circuits, a laboratory evaluation was performed. These tests were designed to measure the performance capabilities of the second-generation system as incorporated in the working model. The system tested was made up of a control unit, a battery module, lead-acid batteries, and an adjustable solar-array simulator. To simulate a typical spacecraft power system configuration, a PWM regulator and load were connected in

parallel with the MPPT as shown in Figure 12. Results of these tests are presented in the following.

Power Transfer Efficiency

The power transfer efficiency is defined as the ratio of average MPPT output power to average input power expressed as a percentage.

$$\eta T = \frac{V_{B_{AVE}} \times I_{B_{AVE}}}{V_{S_{AVE}} \times I_{S_{AVE}}} \times 100. \qquad (8)$$

The efficiency generally exceeded 90 percent as shown in Figure 13. This includes the effects of tracking error, which can be appreciable. Tracking error for the presented data was approximately 10 percent, which reduced the measured efficiency by several percent. For example: at P_S of 260 watts, the power transfer efficiency increased from 90 to 94 percent with
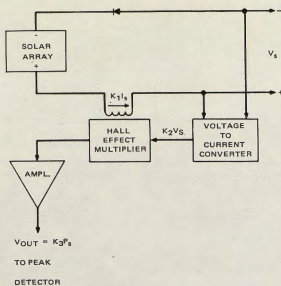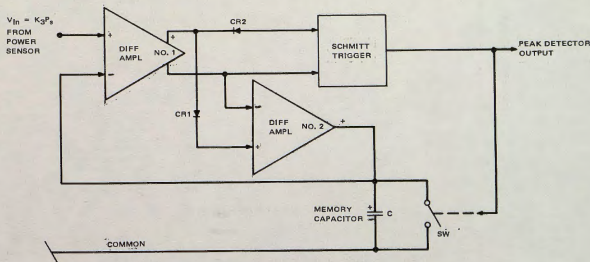
Figure 10. Power Sensor Diagram

Figure 11. Peak Detector Diagram

Trickle Charge Rate Control

The trickle-charge-current-regulation function was set to about 300 milliamperes for the working model. This mode of operation occurs when the battery voltage, battery temperature, or both, exceed safe limits as determined by battery considerations (load protection modes). Non-tracking operation, as occurs in the maximum-charge-current-limit mode, also applies to the trickle-charge-rate controls.

Tracking Error

For the high-speed MPPT, tracking error is best found by comparing the average power delivered by the source (as determined from average voltage and average current meter readings) to the known source power at the maximum power point. Tracking error is directly proportional to the sensitivity of the peak detector circuit, which does not vary as a function of array power level.

the improved (Hall-effect) power sensor/peak detector. The increased tracking error (10 percent) was due to the use of a power sensor/peak detector less sensitive than the improved controls described herein.

Maximum Charge Rate Control

The maximum-charge-current-limit function was set to operate at 11.0 amperes. Limiting action satisfactorily limited the average current which, for a single battery channel system, inhibits the power-maximizing controls.

Average tracking error is defined as:

$$E_T = \frac{P_{max} - P_{S_{ave}}}{P_{max}} \times 100. \qquad (9)$$

The measured tracking error was 1.2 percent at an array maximum power of 285 watts for the Hall-effect power sensor.

Load Transient Susceptibility

Transients were induced at the output of the PWM regulator to ascertain the response of the MPPT
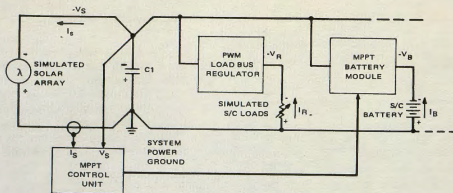
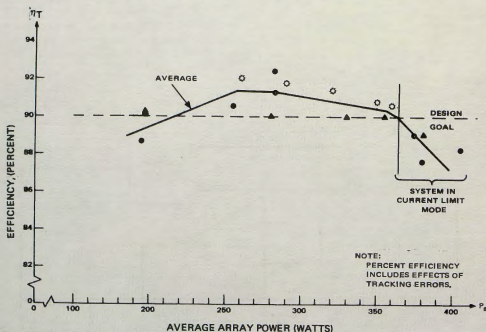Figure 12. MPPT System Test Configuration

Figure 13. High-Speed MPPT Power Transfer Efficiency

controls to load transients. The effect of load transients on the tracking operation was considered for transients of up to 6 amperes. Sometimes, depending on the instant of application of the transient, the system became biased off the source maximum power point, but tracking operation was restored by the pulse absence detector within 2.0 milliseconds. This is a significant improvement over the low-speed system, where the maximum restoring time could be one scanner cycle (about 15 seconds) and a 1-ampere load transient was not tolerable.

Load-MPPT Interaction

When the high-speed MPPT is operated in parallel with the PWM load bus regulator, as in Figure 12, no interaction effects (which cause the disabling of the tracking function) are experienced, as was the case for the low-speed system.

A possible interaction can occur due to the L-C input filter usually used on the PWM regulator. This two-section filter introduces undesirable resonances, which can cause the cessation of tracking operation. This interaction was experimentally verified. Therefore, when a PWM regulator is used in conjunction with the MPPT system, the input filter must be eliminated in order to avoid interactions affecting the tracking mechanism.

Rapidly Varying Solar Array

It was desired to demonstrate the applicability of high-speed MPPT to spacecraft with rapidly varying solar-array characteristics (e.g., spin-stabilized spacecraft with body-mounted solar arrays). Fluctuating array characteristics of this sort are caused by shadowing and variation of the angle-of-incidence of solar energy, both of which primarily affect the short-circuit-current level.

These effects were simulated by sinusoidally varying the short-circuit current of the array simulator. Successful tracking of the maximum power point was maintained for a ±50 percent current variation at frequencies up to 200 Hz, and for a ±20 percent current variation at frequencies up to 1000 Hz.

Thus, the high-speed MPPT has demonstrated not only conceptual feasibility, but applicability to a wide variety of missions.

Summary

As a result of the severe limitations inherent in the first-generation (or low-speed) MPPT system, a second-generation concept was developed to provide a more widely applicable system. The high-speed system retained all the performance features that had been incorporated into the low-speed system.

A working laboratory model of the high-speed MPPT was constructed and evaluated. Laboratory results demonstrated that the basic concept was indeed feasible and that the observed performance was comparable to that of the first generation system. It should be noted that the goal of the working model was to demonstrate feasibility of the concept and that the results are not representative of optimized circuits in an optimum configuration.

The most significant of the results is the elimination of the restrictions of the low-speed system. The presence of load transients and the non-linear input characteristic of a PWM voltage regulator did not cause the MPPT to become biased off the source maximum power point. In addition, the high-speed MPPT system was able to maintain system operation at the maximum power point for a rapidly fluctuating array characteristic (as would be the case for a spin-stabilized spacecraft with a body-mounted solar array).

The second-generation MPPT system provides a means of efficient power conditioning, which can result in significant increases in space power-system capability.

Reference

RCA Astro-Electronics Division, Advanced Voltage Regulator Techniques as Applied to Maximum Power Point Tracking Systems for the Nimbus Meteorological Satellite, Final Report, 16 June 1965 through 10 October 1967, Contract NAS-5-3248, Prepared for NASA-GSFC.